Efficient Coherent Direction-of-Arrival Estimation and Realization Using Digital Signal Processor

Veerendra Dakulagi, *Member, IEEE,* Mukil Alagirisamy, and Mandeep Singh, *Member, IEEE*

***Abstract*— A novel efficient coherent direction-of-arrival (DOA) estimation method is devised in this article. First, a new cost function without the knowledge of source number is developed exploiting the Toeplitz matrices' joint diagonalization structure. Then, the revised steering vectors are used in the place of projection weights of the steering vectors to reconstruct the power spectrum in both noise and signal subspaces. The coherent DOAs are estimated using the 1-D search. Furthermore, the computational complexity of the proposed method is significantly reduced using the Nystrom approximation. Finally, the developed theoretical model is implemented on the TMS320C6678 digital signal processor (DSP) to exemplify the efficacy of the novel method.**

***Index Terms*— Array antenna, coherent signals, digital signal processor (DSP), direction-of-arrival (DOA), Toeplitz matrix.**

I. Introduction

ACCURATE source estimation is one of the key research areas of array signal processing [1]. The direction-of-arrival (DOA) algorithms are responsible for estimating the angle of arrival of the incoming signals and have applications in the localization of sources, detection, and beamforming [2]. A beam-scanning concept is used in the classical methods for direction finding. In this method, each signal power is calculated by scanning a beam through space. The direction with the highest power is considered the angle of arrival of the desired signal. The subspace-based algorithms have high resolution. In this approach, the autocorrelation of a user signal and noise model is formed and are converted into a matrix. The eigenstructures of this matrix are formed and are sorted to give signal and noise subspaces. The subspace-based methods are more accurate and effective for direction finding than the classical methods [3].

The DOA algorithms have been used for source localization in wireless communication [4], sonar [5]–[10], and radar [11]–[13] for many years. Among numerous DOA algorithms, multiple signal classification (MUSIC) [14], [15] and estimation of signal parameters via rotational invariant technique (ESPRIT) [16] are the most widely used methods. In practice, mostly, the source number information is unknown at the receiver. In such cases, an accurate estimation of source number is a difficult task [17].

A beamforming approach such as the Capon-Like [18] may be used to avoid the estimation of the source number. However, it can resolve at most $N/2$ coherent signals in a given uniform linear array (ULA) composed of N sensors if a spatially smoothed covariance matrix is deployed. Nevertheless, it has poor performance in many practical applications due to its low resolution. A preprocessing scheme-based on spatial smoothing (SS) method is presented in [19]. This technique forms subarrays by partitioning the total array. Later, a forward-only spatial smoothing (FOSS) [20] technique was developed, which uses a preprocessing scheme to make the SCM to be full rank. Nevertheless, it deteriorates in performance due to the reduced array aperture. However, this method can manage only at most $N/2$ signals in a ULA with N sensors.

A forward/backward spatial smoothing (FBSS) method was developed in [21] to avoid the aperture loss. However, this approach cannot be applied to resolve the coherent signals. Zhang and Ng [22] presented the MUSIC-like algorithm for DOA estimation. Though this method is more accurate than the classical MUSIC and the Capon-Like, it would not handle the coherent source signals and its performance deteriorates in a low signal-to-noise ratio (SNR) environment. In literature, various well-known DOA methods [23]–[33] including the aforementioned techniques require prior information of the source number for signal estimation. Recently, the ESPRIT-like algorithm presented in [34] resolves the coherent signals. However, this method requires prior information of the source number and presents severe performance degradation for low SNRs and small sample numbers. Recently, Qian *et al.* [35] circumvented these problems. Though this method is superior to the ESPRIT-Like method, it presents a low resolution for certain conditions, has large computational complexity, and needs the following improvements.

1) Practical experiments can be conducted to exemplify the developed hypothetical model.
2) In the problem formulation, the element of the covariance matrix is not derived. A detailed explanation and derivation will make the work more complete and understandable.
3) The computational complexity of this article can be reduced to speed up the algorithm.

In this article, we present a computationally efficient method that is different from [35]. The proposed method provides high resolution for the estimation. We exploit the Nystrom approximation [36] to reduce significantly the computational complexity of the proposed method. Finally, the simulated

Manuscript received March 21, 2019; revised February 16, 2020; accepted March 30, 2020. Date of publication June 4, 2020; date of current version September 3, 2020. *(Corresponding author: Veerendra Dakulagi.)*

Veerendra Dakulagi and Mukil Alagirisamy are with the Department of Electronics and Communication Engineering, Lincoln University College, Kuala Lumpur 47301, Malaysia (e-mail: veerendra.gndec@gmail.com; mukil.a@lincoln.edu.my).

Mandeep Singh is with the Department of Electronics and Communication Engineering, National Institute of Technology Karnataka, Surathkal 575025, India (e-mail: mandeep.singh@nitk.edu.in).

Color versions of one or more of the figures in this article are available online at http://ieeexplore.ieee.org.

Digital Object Identifier 10.1109/TAP.2020.2986045

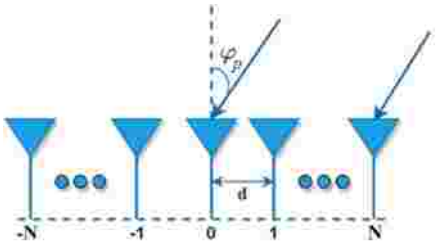

Fig. 1. Considered symmetric ULA model.

results are validated by implementing the proposed method on the TMS320C6678 DSP.

The remainder of this article is organized as follows. In Section II, a considered signal model is explained. Section III presents the proposed technique. Section IV presents the computer simulations, and Section V presents the practical experiment using the TMS320C6778 DSP. Finally, Section VI concludes this article.

II. Array Signal Model

Let us consider a ULA composed of $(2N+1)$ sensors ranging from $(-N,\ldots,0,\ldots,N)$, as shown in Fig. 1. Let $P \leq N$ narrowband signals impinge a ULA from the far-field directions $\varphi_i, i=(1,2,3,\ldots,P)$ and the first L signals are mutually coherent and others are uncorrelated and are independent of the first L signals. Let the time be denoted by the kth sample. The lth coherent source by considering a first source $c_1(k)$ as a reference can be expressed as $c_l(k)=\xi_l[exp(j\partial\Phi_l)]c_1(k), l=2,\ldots,L$. Here, $\partial\Phi_l$ is the phase change and ξ_l is the amplitude fading parameter. Let $\hbar_l=[exp(j\partial\Phi_l)]$ and the signal received at the nth element is $x_n(k)=\sum_{i=1}^{P} c_i(k)exp[-j(2\pi/\lambda)dnsin(\varphi_i)]+n_n(k)$. This expression can also be written as

$$x_n(k)=c_1(k)\sum_{i=1}^{L}\hbar_i exp\left[-j\frac{2\pi}{\lambda}dnsin(\varphi_i)\right] + \sum_{i=L+1}^{P}\hbar_i c_i(k)exp\left[-j\frac{2\pi}{\lambda}dnsin(\varphi_i)\right]+n_n(k). \quad (1)$$

Here, $c_i(k)$ is the ith complex envelope, d is the interelement spacing, λ is the wavelength of a carrier, and $n_n(k)$ is the white Gaussian noise with σ^2 variance and zero mean at the nth element. The observation vector of a ULA is

$$\begin{aligned}\mathbf{x}(k)&=\left[x_{-N}(k),\ldots,x_0(k),\ldots,x_N(k)\right]^T\\&=\mathbf{A}\mathbf{c}(k)\mathbf{A}(k)+\mathbf{N}(k).\end{aligned} \quad (2)$$

Here, $\mathbf{c}(k)=[c_1(k),c_2(k),\ldots,c_P(k)]^T$ is the signal vector, $(\cdot)^T$ is the transpose, and $\mathbf{A}=[\mathbf{a}(\varphi_1),\mathbf{a}(\varphi_2),\ldots,\mathbf{a}(\varphi_P)]$ is the new array manifold vector (AMV) and $\mathbf{a}(\varphi_P)=[exp(j(2\pi/\lambda)dNsin(\varphi_P)),\cdots 1,\ldots,exp(-j(2\pi/\lambda)dNsin(\varphi_P))]^T$ is the $p$thsteering vector. $N(k)$ is the $(2N+1)\times 1$ white Gaussian noise vector.

III. Proposed Algorithm

A. Data Processing and Toeplitz Transformation

According to [34], the output covariance matrix of the observation vector $\mathbf{x}(k)$ is given as $\Re=\Re_{xx}=E[\mathbf{x}(k)\mathbf{x}(k)^H]$. Here, $(\cdot)^H$ is the conjugate transpose and $E\{\}$ is the expectation. Using the results of [34], the derivation to obtain the element of $\Re$ is as follows.

From (1), one has

$$x_n(k)=c_1(k)\sum_{i=1}^{L}\hbar_i exp\left[-j\frac{2\pi}{\lambda}dnsin(\varphi_i)\right] + \sum_{i=L+1}^{P}c_i(k)exp\left[-j\frac{2\pi}{\lambda}dnsin(\varphi_i)\right]+n_n(k). \quad (3)$$

$q(n,\upsilon)$ can be represented using the correlation assumption as $q(n,\upsilon)=E\{\mathbf{x}_n(k)\mathbf{x}_\upsilon^*(k)\}, (n,\upsilon)=-N,\ldots,0,\ldots,N$

$$\begin{aligned}q(n,\upsilon)=&\\&E\left\{\left[c_1(k)\sum_{l=1}^{L}\hbar_l exp(\Psi)+\sum_{l=L+1}^{P}c_l(k)exp(\Psi)+n_n(k)\right]\right.\\&\left.\times\left[c_1^*(k)\sum_{i=1}^{L}\hbar_l^* exp(\Phi)+\sum_{i=L+1}^{P}c_i^*(k)exp(\Phi)+n_{k(k)}^*\right]\right\}\\=&E\{|c_1(k)|^2\}\sum_{l=1}^{L}\hbar_l exp(\Psi)\cdot\sum_{i=1}^{L}\hbar_l^* exp(\Phi)+\sum_{l=1}^{L}\hbar_l exp(\Psi)\\&\cdot\sum_{i=L+1}^{P}E\{c_1(k)c_{i(k)}^*\}exp(\Phi)+\sum_{l=L+1}^{P}E\{c_l(k)c_{1(k)}^*\}exp(\Psi)\\&\cdot\sum_{i=1}^{L}\hbar_i^* exp(\Phi)+\sum_{l=L+1}^{P}\sum_{i=L+1}^{P}E\{c_l(k)c_{i(k)}^*\}exp(\Psi)\\&\cdot exp(\Phi)+\sigma^2\delta_{n,\upsilon}.\end{aligned} \quad (4)$$

In the above expression, we have considered $\Psi=-j(2\pi/\lambda)dnsin(\varphi_l)$ and $\Phi=j(2\pi/\lambda)d\upsilon sin(\varphi_i)$ for the simplification purpose. Suppose that $P_{l,i}=E\{c_l(k)c_i^*(k)\}$, $l,i=1,L+1,\ldots,P$; then, $q(n,\upsilon)$ can also be expressed as

$$\begin{aligned}&q(n,\upsilon)\\&=\sum_{i=1}^{L}\left[P_{1,1}\hbar_i^*\sum_{l=1}^{L}\hbar_l exp(\Psi)+\hbar_i^*\sum_{l=L+1}^{P}P_{l,1}exp(\Psi)\right]\\&\cdot exp(\Phi)+\sum_{i=L+1}^{P}\left[P_{1,i}\sum_{l=1}^{L}\hbar_l exp(\Psi)+\sum_{l=L+1}^{P}P_{l,i}exp(\Psi)\right]\\&\cdot exp(\Phi)+\sigma^2\delta_{n,\upsilon}\end{aligned} \quad (5)$$

$$\begin{aligned}&=\sum_{i=1}^{L}\left[P_{1,1}\hbar_i^*\sum_{l=1}^{L}\hbar_l exp(\Psi)\right]\cdot exp(\Phi)+\sum_{i=L+1}^{P}\left[P_{i,i}exp(-\Phi)\right]\\&\cdot exp(\Phi)+\sigma^2\delta_{n,\upsilon}.\end{aligned} \quad (6)$$

In the previous equation, let

$$b_{n,i} = \begin{cases} P_{1,1}\hbar_i^* \sum_{l=1}^{L} \hbar_l exp(\Psi), & for\ i = 1 \ldots L. \\ P_{i,i} exp(-\Phi), & for\ i = L+1 \ldots P \end{cases} \quad (7)$$

$$q(n, \upsilon) = \sum_{i=1}^{P} b_{n,i} exp(\Phi) + \sigma^2 \delta_{n,\upsilon} = \sum_{i=1}^{P} b_{n,i} exp\left(j\frac{2\pi}{\lambda}\upsilon d sin(\varphi_i)\right) + \sigma^2 \delta_{n,\upsilon} \quad (8)$$

$$\delta_{n,\upsilon} = \begin{Bmatrix} 1, & n = \upsilon \\ 0, & n \neq \upsilon \end{Bmatrix}. \quad (9)$$

Hence, the required Toeplitz matrix [34] can be constructed using the nth row of $\Re$ as

$$\vec{\Re}_n = \begin{bmatrix} q(n,0) & q(n,1) & \ldots & q(n,N) \\ q(n,-1) & q(n,0) & \ldots & q(n,N-1) \\ \vdots & \vdots & \ddots & \vdots \\ q(n,-N) & q(n,-N+1) & \ldots & q(n,0) \end{bmatrix} \quad (10)$$

$$= \mathbf{A}\mathbf{B}_n\mathbf{A}^H + \sigma^2 I_{N+1,n} \quad (11)$$

where $\mathbf{A} = [\mathbf{a}(\varphi_1), \mathbf{a}(\varphi_2), \ldots, \mathbf{a}(\varphi_P)]$ is the new AMV with the pth steering vector being $\mathbf{a}(\varphi_P) = [exp(j(2\pi/\lambda)dNsin(\varphi_P)), \ldots, exp(-j(2\pi/\lambda)dNsin(\varphi_P))]^T$ and $\mathbf{B}_n = diag\{b_{n,1}, \ldots, b_{n,P}\}$ is the pseudosignal covariance matrix.

B. DOA Estimation Without Knowing a Priori Source Number

Let the Toeplitz matrix without noise is given as [35]

$$\vec{\Re}_n = \mathbf{A}\mathbf{B}_n\mathbf{A}^H = \sum_{i=1}^{P} b_{n,i}\mathbf{a}(\varphi_i)\mathbf{a}^H(\varphi_i). \quad (12)$$

Equation (12) has the structure of joint diagonalization. Since $\vec{\Re}_{-n}$ and $\vec{\Re}_n$ have the same statistical data due to the conjugate symmetric nature of the—mth and mth rows in the Toeplitz matrix, it is not necessary to consider all the rows of $(2N+1)$ to construct the Toeplitz matrices [35]. Since the first $(N+1)$ covariance matrix rows have been used without a generality loss, there exist only $(N+1)$ Toeplitz matrices accommodating the useful statistical information. We use these $(N+1)$ Toeplitz matrices to estimate the DOA parameters and identify the range space of the AMV of $\Re$. There exists a vector $\vec{\xi}_P$ for the pth source, which is always orthogonal to the steering vectors expect $\mathbf{a}(\varphi_P)$, that is, $\vec{\xi}_P \perp range[\mathbf{a}(\varphi_1), \mathbf{a}(\varphi_2), \ldots, \mathbf{a}(\varphi_P)]$. Hence, we have

$$\mathbf{a}^H(\varphi_i)\vec{\xi}_P = \begin{cases} \mathbf{a}^H(\varphi_i)\vec{\xi}_P, & for\ i = P \\ 0, & for\ i \neq P. \end{cases} \quad (13)$$

Substituting (13) into (12) yields

$$\vec{\Re}_n\vec{\xi}_P = \sum_{i=1}^{P} b_{n,i}\mathbf{a}(\varphi_i)\mathbf{a}^H(\varphi_i)\vec{\xi}_P = \mu_n\mathbf{a}(\varphi_P). \quad (14)$$

The above expression confirms that $\mathbf{a}(\varphi)$ and $\vec{\Re}_n\vec{\xi}$ are parallel when φ is one of the true DOAs, i.e., $\vec{\Re}_n\vec{\xi} = \mu_n\mathbf{a}(\varphi_P)$ when $-N \leq n \leq 0$. The optimization problem led by the above equation can be given as

$$min_\varphi \mathbf{J}\left(\varphi, \vec{\mu}_n, \vec{\xi}\right) = \sum_{n=-N}^{0} \left\| \vec{\Re}_n\vec{\xi} - \mu_n\mathbf{a}(\varphi) \right\|^2. \quad (15)$$

Here, $\mathbf{J}$ is the exchange matrix. Let its antidiagonal be zero and one elsewhere. $\vec{\xi} \in C^{N+1}$ and $\vec{\mu} = [\mu_{-N}, \ldots, \mu_0]^T \in C^{N+1}$ optimization of (15) by foraging DOAs directly is a complicated process, since $\vec{\xi}$ and $\vec{\mu}$ are unknown. To overcome this difficulty, the cost function of (15) is expanded as

$$\mathbf{J}\left(\varphi, \vec{\mu}_n, \vec{\xi}\right) = \vec{\xi}^H\left[\sum_{n=-N}^{0} \vec{\Re}_n^H\vec{\Re}_n\right]\vec{\xi} - \vec{\xi}^H\left[\sum_{n=-N}^{0} \mu_n\vec{\Re}_n^H\mathbf{a}(\varphi)\right] - \left[\sum_{n=-N}^{0} \mu_n^*\mathbf{a}^H(\varphi)\vec{\Re}_n\right]\vec{\xi} + \mathbf{a}^H(\varphi)\mathbf{a}(\varphi)\sum_{n=-N}^{0}|\mu_n|^2. \quad (16)$$

Let $\mathbf{V} = \sum_{n=-N}^{0} \vec{\Re}_n^H\vec{\Re}_n \in C^{(N+1)(N+1)}$ and $\Im(\varphi) = \left[\vec{\Re}_{-N}\mathbf{a}^H(\varphi), \ldots, \vec{\Re}_0^H\mathbf{a}^H(\varphi)\right] \in C^{(N+1)(N+1)}$. Let us recall that $\sum_{n=-N}^{0} \mu_n = \|\mu\|^2 = 1$ and $\mathbf{a}(\varphi)\mathbf{a}^H(\varphi) = N+1$, (16) can be reexpressed as

$$\mathbf{J}\left(\varphi, \vec{\mu}, \vec{\xi}\right) = \vec{\xi}^H\mathbf{V}\vec{\xi} - \vec{\xi}^H\Im(\varphi)\vec{\mu} - \vec{\mu}^H\Im^H(\varphi)\vec{\xi} + N + 1. \quad (17)$$

Let us differentiate the above equation for fixed φ and $\vec{\mu}$ with respect to $\vec{\xi}$ and consider the resultant equation to zero to get $(\partial\mathbf{J}(\varphi, \vec{\mu}, \vec{\xi}))/(\partial\vec{\xi}) = 2\left(\mathbf{V}\vec{\xi} - \Im(\varphi)\vec{\mu}\right) = 0_{N+1}$. This leads to

$$\vec{\xi}_{opt} = \mathbf{V}^+\Im(\varphi)\vec{\mu}. \quad (18)$$

Let us substitute (18) into (17) to yield

$$min_\varphi \mathbf{J}(\varphi, \vec{\mu}) = N + 1 - \vec{\mu}^H\Im^H(\varphi)\mathbf{V}^+\Im(\varphi)\vec{\mu}. \quad (19)$$

Minimizing the above equation corresponds to maximizing $-\vec{\mu}^H\Im^H(\varphi)\mathbf{V}^+\Im(\varphi)\vec{\mu}$. Let us consider $\sum_{i=1}^{N+1} \lambda_i\mathbf{y}_i\mathbf{y}_i^H$ as the eigenvalue decomposition of $\Im^H(\varphi)\mathbf{V}^+\Im(\varphi)$ with $\lambda_1 \geq \cdots \geq \lambda_{N+1}$ as the eigenvalues and $\{\mathbf{y}_i\}_{i=1}^{N+1}$ as the respective eigenvectors. In the continuation

$$min_\varphi\left\{\vec{\mu}^H\Im^H(\varphi)\mathbf{V}^+\Im(\varphi)\vec{\mu}\right\} = max_\varphi\left\{\sum_{i=1}^{N+1} \lambda_i\left|\vec{\mu}^H\mathbf{y}_i\right|\right\} = \lambda_1. \quad (20)$$

The above expression holds only when $\vec{\mu}$ represents the eigenvectors of $\Im^H(\varphi)\mathbf{V}^+\Im(\varphi)$, that is, $\vec{\mu} = \mathbf{y}_1$ and λ_1 is the maximum eigenvalue. Hence, (19) can be simplified as $min_\varphi\mathbf{J}(\varphi)$. Here, $\mathbf{J}(\varphi) = N + 1 - max\, eig\{\Im^H(\varphi)\mathbf{V}^+\Im(\varphi)\}$. Now, the pseudopower spectrum by Qian *et al.* [35] is given as

$$P(\varphi) = \left[\frac{1}{N + 1 - max\, eig\{\Im^H(\varphi)\mathbf{V}^+\Im(\varphi)\}}\right]. \quad (21)$$

C. Improved Method

In this section, we have improved the method by Qian *et al.* [35] in two stages. In the first stage, the coherent signal sources are estimated without knowing the source number, and in the second stage, we reconstruct a new data matrix in the vicinity of the DOAs estimated in the first stage. We use the new steering vectors obtained to rebuild the received data by projecting the originally collected data. Finally, coherent DOAs can be obtained by a new power spectrum derived. In the first stage, the coherent sources are resolved by the high-resolution estimation using (21). Then, the left-hand and right-hand sides of φ_i are resolved to acquire φ_i^- and φ_{+i}. In the second stage, we construct $\mathbf{W} = \left[\mathbf{a}(\varphi_1^-)\mathbf{a}(\varphi_1)\mathbf{a}(\varphi_1^+), \ldots, \mathbf{a}(\varphi_P^-)\mathbf{a}(\varphi_P)\mathbf{a}(\varphi_P^+)\right]$, which is a steering matrix of size $(2N+1)\times 3P$ to obtain the array output as

$$\mathbf{y}(k) = \mathbf{W}^H\mathbf{x}(k) = \mathbf{W}^H\mathbf{A}\mathbf{c}(k) + \mathbf{W}^H\mathbf{N}(k). \tag{22}$$

The above equation is expressed as

$$\mathbf{y}(k) = \mathbf{A}_N\mathbf{c}(k) + \mathbf{N}_N(k) \tag{23}$$

where $\mathbf{A}_N = \mathbf{W}^H\mathbf{A}$ and $\mathbf{N}_N(k) = \mathbf{W}^H\mathbf{N}(k)$. Now, we exploit the Nystrom approximation [36] to reduce the computational complexity as follows. The sample covariance matrix of $\mathbf{y}(k)$ is obtained as $\Re_{yy} = E[\mathbf{y}(k)\mathbf{y}(k)^H]$.

The eigenvalue decomposition of the matrix $\Re_{yy}$ is performed as

$$\Re_{yy}\mathbf{b}_y = u_y\mathbf{b}_y. \tag{24}$$

Now, a new covariance matrix of $\Re_{xx}$ and $\Re_{yy}$ is obtained as $\Re_{xy} = E[\mathbf{x}(k)\mathbf{y}(k)^H]$. The eigenvalue decomposition of the new covariance matrix $\Re_{xy}$ is obtained as

$$\Re_{xy}\mathbf{b}_y = u_y\mathbf{b}_{ns}. \tag{25}$$

In the above expression, $\mathbf{b}_{ns}$ denotes the approximate principle eigenvector written as

$$\mathbf{b}_{ns} = \begin{bmatrix} \Re_{xy}\mathbf{b}_y \\ \hline \mathbf{u}_y \end{bmatrix}. \tag{26}$$

Now, the approximated signal subspace of the matrix $\Re_{xx}$ is expressed as $\mathbf{E}_{ns} = \left[\mathbf{e}_{ns}^1, \ldots, \mathbf{e}_{ns}^P\right]$, where $\left[\mathbf{e}_{ns}^1, \ldots, \mathbf{e}_{ns}^P\right]$ denotes the approximated principle eigenvectors of $\Re_{xx}$. Finally, the pseudospectrum of the new algorithms is written as

$$P(\varphi)_{improved} = \frac{1}{\mathbf{a}(\varphi)^H\mathbf{E}_{ns}\mathbf{E}_{ns}^H\mathbf{a}(\varphi)}. \tag{27}$$

IV. Results and Discussion

In this section, computer simulations are carried out to evaluate the performance of the proposed DOA estimator and the comparison with other algorithms in terms of SNR, probability of resolution (PR), and root-mean-square error (RMSE) is made. The RMSE is evaluated by applying the Monte Carlo simulation. This is expressed as RMSE $= \sqrt{\sum_{i=1}^{T}(\hat{\varphi}_i - \varphi)^2/(T)}$. Here, $T = 500$ trails, $\hat{\varphi}_i$ represents the true DOA, and φ is the estimated DOA value.

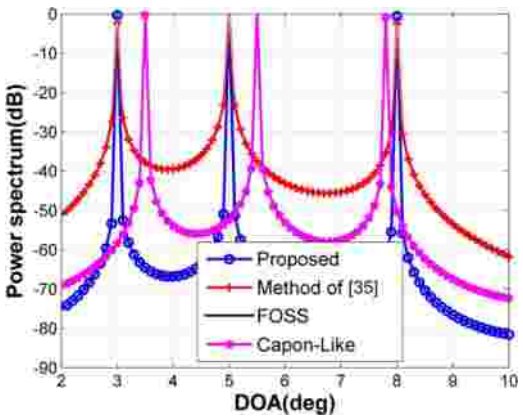

Fig. 2. Spatial spectrum: coherent signals.

A. Spatial Spectrum

Let us consider three signals with equal powers arriving at a five-element ULA from the directions 3°, 5°, and 8°. Let the interelement spacing be $d = 0.5\lambda$, the SNR is set to be 20 dB, and let the sample number be 500. The simulation result of this example is shown in Figs. 2 and 3 when the received signals are coherent and uncorrelated. In Fig. 2, it is noted that the Capon-Like beamformer presents incorrect estimation whereas the proposed method has three clear peaks. This confirms that, for a five-element ULA, the proposed algorithm has the potential to resolve at the most three accurate coherent signals. The pseudospectrum obtained for all the uncorrelated signals is shown in Fig. 3. The FOSS, the method from [35], and the Capon-Like techniques do not require the SS for this case. Among all four methods, the Capon-Like method exhibits the worst performance.

B. RMSE Versus SNR

The performance of the RMSE as a function of the SNR is examined in this example. Consider two uncorrelated sources impinging a nine-element ULA from the directions $-25.5°$ and 10°, and two coherent signals are arriving from 45° and 15°. Let the number of samples be $M = 100$ and 500 Monte Carlo trials for each SNR. The computer simulation of this example is shown in Fig. 4. It is seen that the estimation accuracy of the ESPRIT-like algorithm is the worst and the performance of the proposed method is the best.

C. PR Versus SNR

Let us study the performance of the PR as a function of SNR in this example, keeping all the parameters unchanged. The computer simulations in Fig. 5 depict that the ESPRIT-like algorithm attains full (100%) PR by increasing slowly when the SNR is greater than 25 dB. The proposed method achieves full PR when the SNR = 0 dB. However, the two remaining methods obtain 100% PR when the SNR > 5 dB.

D. RMSE and PR Versus M

Let us now examine the performances of RMSE and PR versus sample size. The SNR is fixed to be 10 dB, keeping

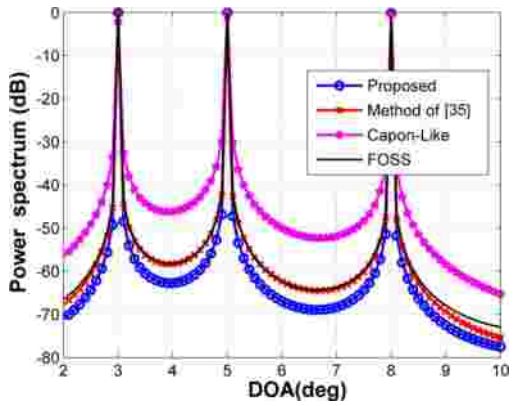

Fig. 3. Spatial spectrum: uncorrelated signals.

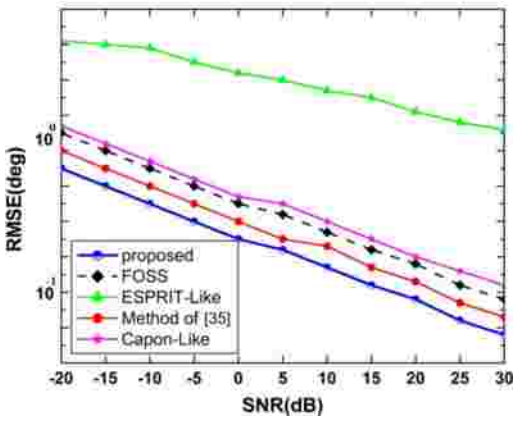

Fig. 4. RMSE versus SNR.

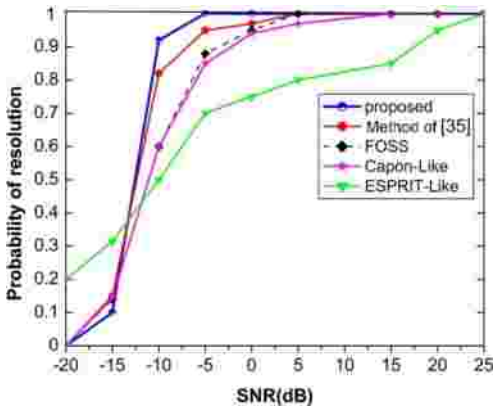

Fig. 5. PR versus SNR.

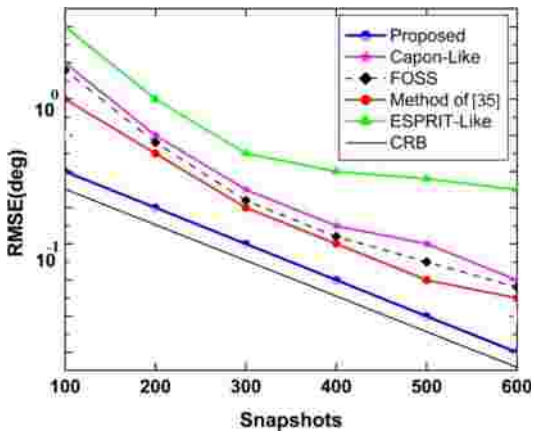

Fig. 6. RMSE versus snapshots.

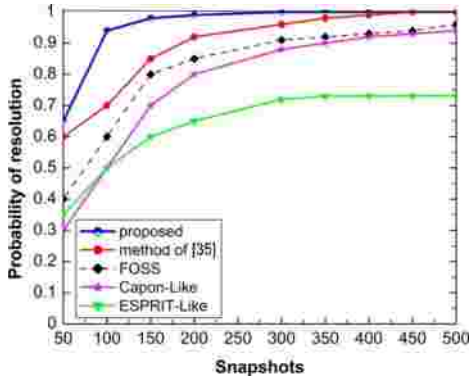

Fig. 7. PR versus snapshots.

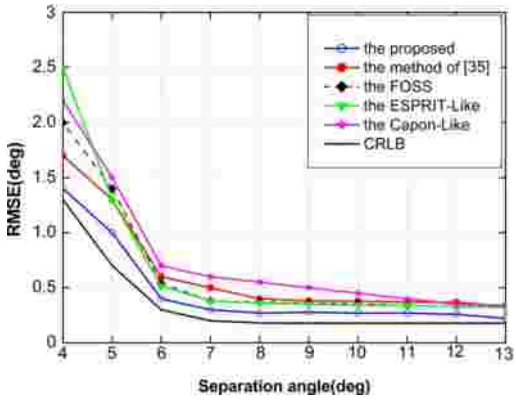

Fig. 8. RMSE against separation angle.

the other parameters unchanged. The simulation results of this example are demonstrated in Fig. 6. It is noted that the RMSE performance of the proposed approach is much better than that in [24]. Nevertheless, the method by Qian *et al.* [35] is superior to the Capon-Like, the FOSS, and the ESPRIT-Like algorithms for all the values of M. Similar observations are marked from Fig. 7.

E. RMSE Versus Separation Angle

The RMSE performance as a function of separation angle is presented. In this experiment, we consider the ULA that consists of six antennas receiving two coherent sources from the directions $10°$ and $10° + \Delta\varphi$. We set the SNR and snapshots to 15 dB and 250, respectively, and the step size $\Delta\varphi$ is $1°$. The computer simulation demonstrated in Fig. 8 shows that the proposed method has superior RMSEs performance when the separation angle is $4°$. However, the performances of the Capon-Like and ESPRIT-Like methods are unsatisfactory.

F. Analysis of Computational Complexity

The complexity of the DOA estimators is illustrated by considering the average CPU time taken by all the algorithms for the DOA estimation. We use the reduced running time Monte Carlo simulations to analyze the simulation (average CPU) times of all four algorithms. This is expressed

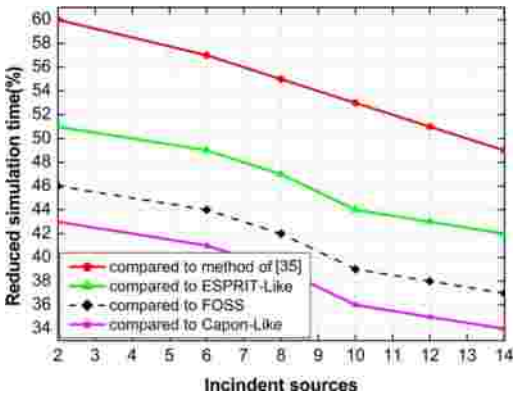

Fig. 9. Reduced simulation time (in %) versus incident signals.

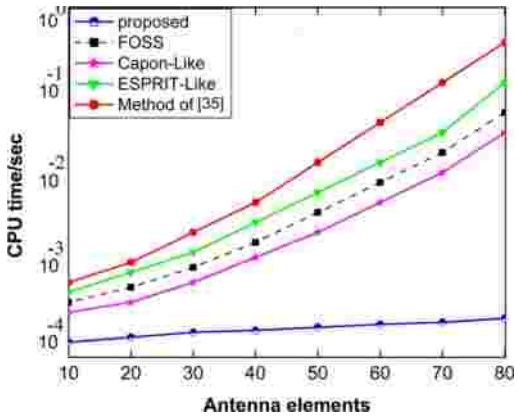

Fig. 10. CPU time versus array elements.

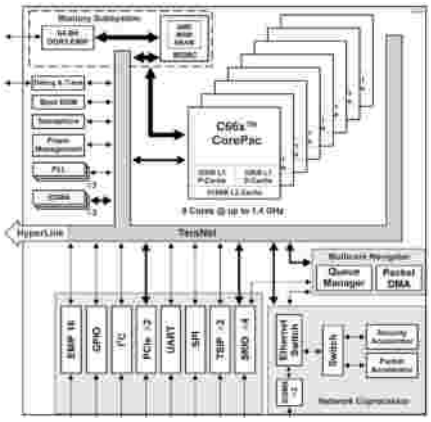

Fig. 11. Functional block diagram of the TMS320C6678 device.

by $T = \left[(T_{pre} - T_{new}/T_{pre})\right] \times 100\%$, where T_{pre} and T_{new}, respectively, are the previous and new (proposed) methods' averaged Monte Carlo simulation times. In this experiment, we assume two far-field signals located at 20° and 60°. We deem a six-element array separated by d $= 0.5\lambda$. The snapshots and SNR are set to be 200 and 20 dB, respectively. The percentage of the reduced simulation time for several incident sources using 500 Monte Carlo trials is illustrated in Fig. 9. The computer simulations presented in Fig. 9 illustrate that the reduced simulation time dramatically decreases as the number of sources increases. When the incident signals are four, the reduced simulation times in percentage compared with the proposed method are respectively 59%, 50%, 45%, and 42% for the Qian *et al.* [35], ESPRIT, FOSS, and Capon-Like methods. This proves that the speed of the proposed method is very high compared with the remaining methods. Fig. 10 shows the CPU times in second for the proposed, the method of [35], the Capon-Like, the ESPRIT-like, and the FOSS methods. In this experiment, we set $M = 100$ and $P = 3$, and the signal sources are considered randomly from $-90°$ to 90°. The antenna elements are varied from 10 to 80. An Intel-*i*3 personal computer with 3.3 GHz is used to obtain the average CPU time requirement of each method. Here, the MATLAB functions *tic* and *toc* are used to record the CPU time in second. From the computational time plot, one can note that the proposed method has the highest speed, since it uses the Nystrom method [36] to reduce the computational complexity. Meantime, the method in [35] exhibits poor performance compared with all the methods.

V. Implementation of the Proposed Method

In recent years, hardware design for the estimation of DOAs is put into practice using different versions of the digital signal processors (DSPs). Among all the DSP processors, the TMS320C6678 is the highest floating and fixed-point processor. It is based on the Texas instrumentation's (TI) keystone multicore architecture. The TMS320C6678 processor integrates a large amount of on-chip memory. It has a development tool that includes a windows debugger interface, an enhanced *C* compiler, an assembling optimizer, and so on. The C6678 DSP consists of two register files, two data paths, and eight functional units. Incorporating eight C66x DSP cores, this device can run at a core speed of up to 1.4 GHz. TI's C6678 DSP offers about 11.2 GHz cumulative digital signal processing for a broad range of applications. The block diagram of the TMS320*C*6678 device is shown in Fig. 11. The C66x core device has $4\times$ the multiply accumulative (MAC) capacity and 90 new instructions of its previous version targeted for vector math-oriented processing and floating-point capacities. Through the use of TIś C/C++ compiler, a very high level of parallelism can be achieved. For the realization of the proposed method using a DSP C6678, let us consider a symmetric ULA composed of five sensors. Let three narrowband signals impinge a ULA from the far-field directions $-60°$, 0°, and 40°. Let the interelement spacing be d $= 0.5\lambda$, the SNR is set to be 20 dB, and let the sample number be 500. The experimental setup is shown in Fig. 12. In this experiment, the latest SIMD technique is adapted from the DSP C6678. The performance of the proposed method is evaluated using the TMS320C6678 DSP with an XDS560v2 emulator and a code composer studio CCS5.3 software platform. Consider that the *a priori* information of the source number is not known for the proposed method.

We have to compute the value of pseudopower spectrum P at each point (φ). Suppose the value of φ is varying from $-90°$ to 90° with the interval of 1°, it is required to compute the value of P for $(91 * 181)$ times. For each pseudopower spectrum iteration, it gives rise to three complex matrix multiplications. Here, each matrix multiplication can

Fig. 12. Experimental setup for DOA estimation.

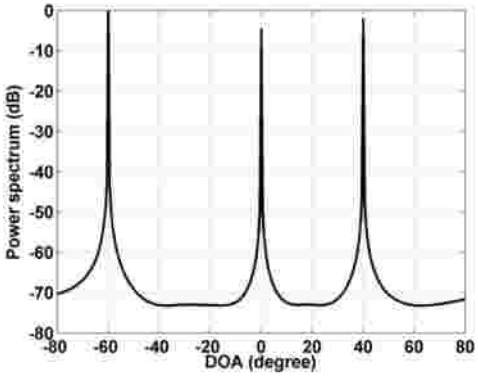

Fig. 13. DOA estimation using C6678 DSP.

be deemed as independent MACs. The process of estimation induces a huge number of MACs. As the DSP C6678 executes instructions on 128-bit vectors, we consider four single-precision floating-point MACs in an SIMD manner to enhance the performance. The pseudopower spectrum of the proposed method for the aforementioned DOAs is obtained in Fig. 13. The DOAs from -90° to 90° with the interval of 1° are scanned in this experiment.

VI. Conclusion

In this article, an efficient method for the estimation of coherent DOAs is presented and a practical realization using a TMS320*C*6678 DSP is carried out. The most significant advantage of the proposed work is that it does not require prior information of the source number for the estimation. The simulated results confirm that the proposed method offers the high-resolution DOA estimation with reduced simulation time compared with other methods, that is, the proposed method with about 59%, 50%, 45%, and 42% decreased the CPU time, respectively, of the Qian *et al.* [35], the ESPRIT-Like, the FOSS, and the Capon-Like methods can offer the same resolution efficacy. Both the simulated results and the practical realization confirm the effectiveness of the new method.

References

[1] H. Krim and M. Viberg, "Two decades of array signal processing research: The parametric approach," *IEEE Signal Process. Mag.*, vol. 13, no. 4, pp. 67–94, Jul. 1996.

[2] R. Kumaresan and D. W. Tufts, "Estimating the angles of arrival of multiple plane waves," *IEEE Trans. Aerosp. Electron. Syst.*, vol. AES-19, no. 1, pp. 134–139, Jan. 1983.

[3] G. Xu and T. Kailath, "Fast subspace decomposition," *IEEE Trans. Signal Process.*, vol. 42, no. 3, pp. 539–551, Mar. 1994.

[4] V. Dakulagi and M. Bakhar, "Smart antenna system for DOA estimation using single snapshot," *Wireless Pers. Commun.*, vol. 107, no. 1, pp. 81–93, Jul. 2019.

[5] W.-Q. Wang, "Overview of frequency diverse array in radar and navigation applications," *IET Radar, Sonar Navigat.*, vol. 10, no. 6, pp. 1001–1012, Jul. 2016.

[6] I. Bekkerman and J. Tabrikian, "Target detection and localization using MIMO radars and sonars," *IEEE Trans. Signal Process.*, vol. 54, no. 10, pp. 3873–3883, Oct. 2006.

[7] J. Steinwandt, F. Roemer, and M. Haardt, "Generalized least squares for ESPRIT-type direction of arrival estimation," *IEEE Signal Process. Lett.*, vol. 24, no. 11, pp. 1681–1685, Nov. 2017.

[8] G. Zheng and B. Chen, "Unitary dual-resolution ESPRIT for joint DOD and DOA estimation in bistatic MIMO radar," *Multidimensional Syst. Signal Process.*, vol. 26, no. 1, pp. 159–178, Jan. 2015.

[9] S.-D. Kim, Y. Ju, and J.-H. Lee, "Design and implementation of a full-digital pulse-Doppler radar system for automotive applications," in *Proc. IEEE Int. Conf. Consum. Electron. (ICCE)*, Jan. 2011, pp. 563–564.

[10] Veerendra, M. Bakhar, and R. M. Vani, "Robust blind beam formers for smart antenna system using window techniques," *Procedia Comput. Sci.*, vol. 93, pp. 713–720, Jan. 2016.

[11] A.-A. Saucan, T. Chonavel, C. Sintes, and J.-M. Le Caillec, "CPHD-DOA tracking of multiple extended sonar targets in impulsive environments," *IEEE Trans. Signal Process.*, vol. 64, no. 5, pp. 1147–1160, Mar. 2016.

[12] Y. Liu and H. Cui, "Antenna array signal direction of arrival estimation on digital signal processor (DSP)," *Procedia Comput. Sci.*, vol. 55, pp. 782–791, Jan. 2015.

[13] L. Osman, I. Sfar, and A. Gharsallah, "The application of high-resolution methods for DOA estimation using a linear antenna array," *Int. J. Microw. Wireless Technol.*, vol. 7, no. 1, pp. 87–94, Feb. 2015.

[14] R. Schmidt, "Multiple emitter location and signal parameter estimation," *IEEE Trans. Antennas Propag.*, vol. AP-34, no. 3, pp. 276–280, Mar. 1986.

[15] Veerendra, M. Bakhar, R. M. Vani, and P. V. Hunagund, "Implementation and optimization of modified MUSIC algorithm for high resolution DOA estimation," in *Proc. IEEE Int. Microw. RF Conf.*, Dec. 2014, pp. 190–193.

[16] R. Roy and T. Kailath, "ESPRIT-estimation of signal parameters via rotational invariance techniques," *IEEE Trans. Acoust., Speech, Signal Process.*, vol. 37, no. 7, pp. 984–995, Jul. 1989.

[17] A. L. Swindlehurst and T. Kailath, "A performance analysis of subspace-based methods in the presence of model errors, Part I: The MUSIC algorithm," *IEEE Trans. Signal Process.*, vol. 40, pp. 1758–1774, Jul. 1992.

[18] R. Sanudin, N. H. Noordin, A. O. El-Rayis, N. Haridas, A. T. Erdogan, and T. Arslan, "Capon-like DOA estimation algorithm for directional antenna arrays," in *Proc. Loughborough Antennas Propag. Conf.*, Loughborough, U.K., 2011, pp. 1–4, doi: 10.1109/LAPC.2011.6114042.

[19] J. E. Evans, J. R. Johnson, and D. F. Sun, "Application of advanced signal processing technique to angle of arrival estimation in ACT navigation and surveillance systems," MIT Lincoln Lab., Lexington, MA, USA, Tech. Rep. 582, 1982.

[20] T. J. Shan, M. Wax, and T. Kailath, "On spatial smoothing for direction-of-arrival estimation of coherent signals," *IEEE Trans. Acoust., Speech, Signal Process.*, vol. ASSP-33, no. 4, pp. 806–811, Aug. 1985.

[21] S. U. Pillai and B. H. Kwon, "Forward/backward spatial smoothing techniques for coherent signal identification," *IEEE Trans. Acoust., Speech, Signal Process.*, vol. 37, no. 1, pp. 8–15, Jan. 1989.

[22] Y. Zhang and B. P. Ng, "MUSIC-like DOA estimation without estimating the number of sources," *IEEE Trans. Signal Process.*, vol. 58, no. 3, pp. 1668–1676, Mar. 2010.

[23] S. Durrani and M. E. Bialkowski, "Effect of mutual coupling on the interference rejection capabilities of linear and circular arrays in CDMA systems," *IEEE Trans. Antennas Propag.*, vol. 52, no. 4, pp. 1130–1134, Apr. 2004.

[24] L. C. Godara, "Application of antenna arrays to mobile communications. II. Beam-forming and direction-of-arrival considerations," *Proc. IEEE*, vol. 85, no. 8, pp. 1195–1245, Aug. 1997.

[25] V.-K. Mai, D. Pastor, A. Aissa-El-Bey, and R. Le-Bidan, "Robust estimation of non-stationary noise power spectrum for speech enhancement," *IEEE/ACM Trans. Audio, Speech, Lang. Process.*, vol. 23, no. 4, pp. 670–682, Apr. 2015.

[26] Z. Tan and A. Nehorai, "Sparse direction of arrival estimation using co-prime arrays with off-grid targets," *IEEE Signal Process. Lett.*, vol. 21, no. 1, pp. 26–29, Jan. 2014.

[27] I. Bilik, "Spatial compressive sensing for direction-of-arrival estimation of multiple sources using dynamic sensor arrays," *IEEE Trans. Aerosp. Electron. Syst.*, vol. 47, no. 3, pp. 1754–1769, Jul. 2011.

[28] L. Qiu, Y. Cai, R. C. de Lamare, and M. Zhao, "Reduced-rank DOA estimation algorithms based on alternating low-rank decomposition," *IEEE Signal Process. Lett.*, vol. 23, no. 5, pp. 565–569, May 2016.
[29] B. Porat and B. Friedlander, "Analysis of the asymptotic relative efficiency of the MUSIC algorithm," *IEEE Trans. Acoust., Speech, Signal Process.*, vol. ASSP-36, no. 4, pp. 532–544, Apr. 1988.
[30] B. P. Ng, M. H. Er, and C. Kot, "A MUSIC approach for estimation of directions of arrival of multiple narrowband and broadband sources," *Signal Process.*, vol. 40, no. 2, pp. 319–323, 1994.
[31] X. Mestre and M. Á. Lagunas, "Modified subspace algorithms for DoA estimation with large arrays," *IEEE Trans. Signal Process.*, vol. 56, no. 2, pp. 598–614, Feb. 2008.
[32] M. Haardt and A. N. Josef, "Unitary ESPRIT: How to obtain increased estimation accuracy with a reduced computational burden," *IEEE Trans. Signal Process.*, vol. 43, no. 5, pp. 1232–1242, May 1995.
[33] A. Paulaj, R. Roy, and T. Kailath, "Estimation of signal parameters via rotational invariance techniques-ESPRIT," in *Proc. 19th Asilomar Conf. Signals, Syst. Comput.*, Pacific Grove, CA, USA, Nov. 1985, p. 8389.
[34] F.-M. Han and X.-D. Zhang, "An ESPRIT-like algorithm for coherent DOA estimation," *IEEE Antennas Wireless Propag. Lett.*, vol. 4, pp. 443–446, 2005.
[35] C. Qian, L. Huang, W.-J. Zeng, and H. C. So, "Direction-of-arrival estimation for coherent signals without knowledge of source number," *IEEE Sensors J.*, vol. 14, no. 9, pp. 3267–3273, Sep. 2014.
[36] G. Liu, H. Chen, X. Sun, and R. C. Qiu, "Modified MUSIC algorithm for DOA estimation with Nyström approximation," *IEEE Sensors J.*, vol. 16, no. 12, pp. 4673–4674, Jun. 2016.

Veerendra Dakulagi (Member, IEEE) received the B.E degree in electronics and communication engineering, the M.Tech. degree in power electronics, and the Ph.D. degree in array signal processing from the Visvesvaraya Technological University, Belgaum, India, in 2007, 2011, and 2018, respectively.

He is currently a Post-Doctoral-Fellow with the Lincoln University College, Kuala Lumpur, Malaysia. He has published over 30 technical journals (including IEEE transactions, IEEE journals, Elsevier, Springer, and Taylor & Francis) and one patent in array signal processing.

Dr. Dakulagi has received many awards in education, including the Award for Research Publications by the Vision Group on Science and Technology, Government of Karnataka, India, under the leadership of Bharat Ratna Prof. C.N.R. Rao, and the Best Teacher/Researcher Award by the Guru Nanak Dev Engineering College, Bidar, for the academic year 2018–2019. He is the Editor-in-Chief of the *Journal of Advanced Research in Wireless, Mobile & Telecommunication* and the *Journal of Advanced Research in Signal Processing & Applications*. He also serves as an Associate Editor for the *Journal on Communication Engineering and Systems* and the *Journal on Electronics Engineering*. He is a Regular Reviewer to various IEEE transactions/journals, Elsevier, Taylor & Francis, Springer journals, and International Conferences.

Mukil Alagirisamy received the Ph.D. degree in engineering from the Lincoln University College, Kuala Lumpur, Malaysia, in 2012.

She has completed her PDF in 2015. She is currently working as an Assistant Professor and a Coordinator for Master of Science in Electrical, Electronics and Telecommunication Engineering Programs at the Lincoln University College. Her research interests are in sink mobility patterns, clustering, modulation, data aggregation, and compressive sensing techniques for wireless sensor networks.

Mandeep Singh (Member, IEEE) received the Ph.D. degree in electronics and communication engineering from IIT Roorkee, Roorkee, India, in 2018.

He is currently working as an Assistant Professor with the Department of Electronics and Communication Engineering, National Institute of Technology Karnataka, Surathkal, India. His current research interests include digital signal processing, nanophotonics devices, and optical sensors.